J. mar. biol. Ass. India, 1972, 14 (1): 61-83

SOUND VELOCITY STRUCTURE OF THE NORTHWEST INDIAN OCEAN*

DON F. FENNER AND PAUL J. BUCCA

U.S. Naval Oceanographic Office, Washington D.C., U.S.A.

ABSTRACT

Analysis of historical sound velocity and temperature-salinity data north of 10°S latitude and west of 80°E longitude indicates that mixing of relatively warm, saline Red Sea and Persian Gulf Intermediate Waters with relatively cold, dilute Subtropical Subsurface and Antarctic Intermediate Waters results in an extremely strong negative velocity gradient to about 200 meters, sporadic sound velocity perturbations above primary axial depth, and a wide, depressed primary sound channel. Perturbations in the sound velocity structure above primary axial depth were found more than 80% of the time throughout much of the Somali Basin, with minima associated with low salinity cores and maxima associated with high salinity cores. A meaningful upper sound channel was found west and south of Socotra and in a pocket northeast of Zanzibar associated with intrusions of Red Sea Intermediate and Subtropical Subsurface Waters, respectively. The absence of a widespread upper sound channel in the Northwest Indian Ocean is attributable to the lack of sufficient cold, dilute water north of the equator and to intensive mixing of the four intrusive high and low salinity water masses, particularly in the Somali Basin.

In the region north of about 8°N latitude, primary axial depths are anomalously deep (greater than 1700 meters) and primary axial velocities are anomalously high (greater than 1496 meters/second) in the presence of high concentrations of Red Sea and/or Persian Gulf Intermediate Waters. Areal patterns of both variables show the preferential flow of Red Sea Intermediate Water along the African coast and a zone of relatively rapid transition south of the equator that corresponds to the limit of persistent Antarctic Intermediate Water occurrence. During the northeast (winter) monsoon, deeper critical depths are found throughout the Somali Basin due to southward transport of higher temperature and salinity waters from the Arabian Sea by the Northeast Monsoon Current. During the southwest (summer) monsoon, anomalously shallow critical depths are found in association with two widespread centers of upwelling along the Somali and Muscat-Oman coast. Seasonally reversing monsoons do not appreciably affect the sound velocity structure below 200 meters, except in centers of upwelling. Rather, intensive mixing between the four intrusive water masses is the predominate cause of the complex and irregular sound velocity structure and extremely broad primary sound channel found throughout the Northwest Indian Ocean.

INTRODUCTION

DESPITE the large body of data collected by the International Indian Ocean Expedition (IIOE), no comprehensive study of the sound velocity structure of any region of the Indian Ocean has yet appeared in the literature. In an effort to correct this discrepancy, the authors have analyzed all available historical data in the Northwest Indian Ocean (north of 10°S latitude and west of 80°E longitude) in terms of sound velocity structure. In this area, various environmental factors cause the formation of a sound velocity structure that consists of a surface mixed layer and an extremely strong negative velocity gradient to about 200 meters, an essentially

* Presented at the 'Symposium on Indian Ocean and Adjacent Seas—Their Origin, Science and Resources' held by the Marine Biological Association of India at Cochin from January 12 to 18, 1971.

isovelocity layer to the approximate depth of the high salinity core, a weak negative gradient to primary axial depth, and a positive gradient from primary axial depth to the bottom. This paper seeks to determine and define the temporal and spatial distribution of this anomalous sound velocity structure in terms of temperature-salinity (T-S) relationships, water mass analysis, and existing circulation patterns. The locations of all sound velocity and/or T-S profiles cited herein are shown on Figure 4. The actual profiles are presented in the Appendix.

Sources and Treatment of Data

All available sound velocity-depth profiles from the archives of the National Oceanographic Data Center (NODC), Washington, D.C. (World Data Center A) were analyzed during the preparation of this paper. These profiles were available to the authors in the form of monthly and seasonal one-degree square sound velocity summaries that contained all Nansen cast and salinity-temperature-depth recorder data extending deeper than 50 meters processed by NODC as of 30 June 1969. These data were converted into sound velocity profiles using the equation of Wilson (1960). In addition, the authors analyzed core salinities for nearly 400 T-S profiles drawn from various IIOE data in order to determine causes of various sound velocity structures and the circulation of various high and low salinity water masses encountered in the area.

Sound velocity data were analyzed for depth and axial velocity of the primary sound channel, the depth and velocity of perturbations lying above primary axial depth, and critical depth, and were compiled by one-degree square and season. For purposes of this paper primary axial depth is defined as the depth of the deepest sound velocity minimum (generally absolute minimum). Sound velocity perturbations are defined as changes from a negative to a positive sound velocity gradient, or vice versa. Critical depth is that depth where the sound velocity is equal to the maximum sound velocity found at the surface or in the surface mixed layer. One-degree square compilations were averaged by two-degree square (i.e., four one-degree squares) on a seasonal basis in the case of critical depth and on an annual basis in the case of primary axial depth, primary axial velocity, and depth and velocity of perturbations above primary axial depth. Two-degree square averages of these parameters then were either contoured or generalised on an areal basis. The two seasons of winter (November through April) and summer (May through October) are used in this paper. These seasons correspond to the maximum duration of the northeast and southwest monsoons, respectively. It is realised, however, that April-May and October-November often are representative of inter-monsoonal periods, and this fact has been taken into account during data analysis. Because of their dependancy upon the seasonally reversing monsoon winds, the two seasons of winter and summer will be referred to throughout the remainder of this paper as the northeast monsoon and the southwest monsoon, respectively. Generally, these two seasons are applicable throughout the entire area.

Generalised Oceanography of the Northwest Indian Ocean

A. *Surface Circulation and Upwelling :*

For purposes of this discussion, the authors have adopted the generalised monsoonal circulation of Matthews (Oct. 1967). During the northeast monsoon, surface circulation is essentially counter clockwise and consists of the Northeast

Monsoon Current flowing out of the Arabian Sea, the North Equatorial Current flowing into the area from the east at about 5°N latitude, and the return Equatorial Countercurrent at about 5°S latitude formed by the above two currents in the Somali Basin. During the southwest monsoon, the surface circulation is reversed and replaced by the strong Somali Current system flowing north along the African Coast. The Somali Current reaches speeds in excess of 6 knots (Swallow and Bruce, 1966) before turning to the east to form the return Southwest Monsoon Current that flows southeast across the area. North and east of Socotra, the southern Arabian Sea is dominated by a series of clockwise gyres during the southwest monsoon. During both monsoons, the South Equatorial Current flows to the west along the southern boundary of the area. The seasonal reversal in surface circulation has definite effects on water properties throughout the region south of about 10°N latitude. During the northeast monsoon, higher salinity waters are brought into this region from the Arabian Sea by the Northeast Monsoon Current ; while during the southwest monsoon, lower salinity waters are brought into this region by a combination of the South Equatorial, Somali, and Southwest Monsoon Currents. North of about 10°N latitude, salinities in the upper 150 to 200 meters of the water column generally are greater than 35.8‰ during both monsoons due to an excess of evaporation over precipitation, except in the presence of upwelling. Upwelling has been documented during the southwest monsoon by Warren, *et al.* (1966) off the Somali coast and by Ryther and Menzel (1965) off the Muscat and Oman coast. Both regions of upwelling have marked influences on surface and near-surface T-S characteristics as well as on sound velocity profiles. These effects seem to be most pronounced off the Somali coast (Fig. A-4).

B. *Circulation of High Salinity Intermediate Waters :*

Two of the five high salinity water masses defined by Rochford (1964) lie sufficiently deep to effect the shape of the sound velocity profile ; those formed in the Persian Gulf and the Red Sea. Persian Gulf Intermediate Water (PGIW) enters the Gulf of Oman through the Strait of Hormuz and spreads throughout the Arabian Sea (north of about 10°N latitude) at depths between 250 and 300 meters. PGIW is also found along the Somali and Indian coasts south to about 5°N latitude during both monsoons. Although substantial quantities of PGIW enter the Gulf of Oman due to the lack of sill in the Strait of Hormuz (La Violette and Frontenac, Aug. 1967), the PGIW salinity maximum is rapidly dissipated in the central Arabian Sea (compare T-S profiles shown on Figs. A-1 and A-2). Larger concentrations of this water mass may be carried farther to the south during the northeast monsoon, but present data are inadequate to determine seasonal flow diagrams.

Red Sea Intermediate Water (RSIW) enters the Gulf of Aden through Bab el Mandeb and spreads throughout most of the area at depths ranging from 500 meters at 20°N to 1000 meters at 10°S latitude. RSIW is absent only in the northern Arabian Sea, east of the Maldive Islands, and in the far southeastern corner of the area. Due to the shallow sill depth across Bab el Mandeb, RSIW is substantially mixed before it enters the Gulf of Aden (La Violette and Frontenac, Aug. 1967). The authors found only 35% unmixed RSIW some 200 nautical miles east of Bab el Mandeb, whereas more than 95% unmixed, high salinity Mediterranean Intermediate Water was found some 250 miles west of the Straits of Gibraltar (Fenner and Bucca, Dec. 1969). Rapid dilution of RSIW continues in the Gulf of Aden, and concentrations greater than 25% rarely are found south or east of Socotra. Although RSIW was found throughout most of the area, a preferential flow of this water mass was found along the African coast. Larger or equal concentrations of RSIW were found during the northeast monsoon throughout the area. This was even the case in the Gulf of Aden (compare seasonal RSIW concentrations on Fig. A-3). A seasonal reversal in the direction of RSIW flow may take place in the northern Somali Basin (as postulated by Warren, *et al.*, 1966), but present data are inadequate for such a definition.

C. *Circulation of Low Salinity Intermediate Waters :*

The Northwest Indian Ocean also is influenced by two flows of low salinity water originating in the South Indian Ocean. According to Ivanenkov and Gubin (1960), intermediate waters of the South Indian Ocean consist of two separate water masses : Antarctic Intermediate Water (AAIW) formed at Sub-antarctic Circumpolar Convergence and Subtropical Subsurface Water (SSW) formed at the Subtropical Convergence (approximately 40°S latitude). AAIW is characterised by a salinity minimum throught the Indian Ocean, whereas SSW is characterised by an oxygen maximum in a layer of decreasing salinity. Although a preferential flow of AAIW and SSW into the area might be expected during the southwest monsoon, present data are inadequate to substantiate such a flow. Rather, the flow of both water masses becomes shoaler and increasingly sporadic to the north during both monsoons.

SSW enters the area along the entire southern boundary and flows north in a layer between PGIW and RSIW (about 400 to 800 meters). As SSW comes into contact with increasing concentrations of RSIW, a salinity minimum is formed at a depth somewhat deeper than that of the characteristic SSW oxygen maximum (e.g., see Fig. A-5). Between about 5° and 10°N latitude, SSW sporadically mixes and interfingers with PGIW and effectively blocks the southward flow of this high salinity water mass. However, in this same region, SSW is mixed out by a combination of PGIW and RSIW.

AAIW also enters the area from the south, and flows north in a layer between about 750 and 1300 meters. However, unlike SSW, most of the AAIW enters the area east of the Seychelles Islands. The land mass effect of the Seychelles Islands apparently causes a bifurcation in AAIW flow, leading to a northward flow of this water mass off the African Coast (under the preferential RSIW flow). Relatively unmixed AAIW was found only in the region south of about 5°S latitude and east of the Seychelles Islands (Fig. A-8). Between about 5°S and 10°N latitude, AAIW sporadically mixes and interfingers with high salinity RSIW advancing from the north. This interfingering is particularly apparent in the Somali Basin, as noted by Warren, *et al.* (1966). Figures A-6 and A-7 show examples of interfingering AAIW and RSIW in the Somali Basin. In the opinion of the authors, AAIW does not flow north between the PGIW and RSIW high salinity cores as postulated by Rochford (1966), but rather interfingers with RSIW below the 27.0 to 27.2 sigma-T surfaces as postulated by Warren, *et al.* (1966).

D. *Water Masses and T-S Relationships :*

Figure 1 shows a composite of T-S relationships and defines water masses found in the area. Indian Equatorial Water (IEW) is the predominate surface and nearsurface water mass encountered in the Northwest Indian Ocean south of about 8°N latitude. IEW is circulated throughout this region by the North Equatorial Current and the Equatorial Countercurrent during the northeast monsoon and by the Somali and Southwest Monsoon Currents during the southwest monsoon. This water mass apparently is formed during both monsoons along a weak front at about 6° to 7°N latitude due to mixing of low salinity water carried by the South Equatorial Current with higher salinity water from the north (Scherbinin, 1969).

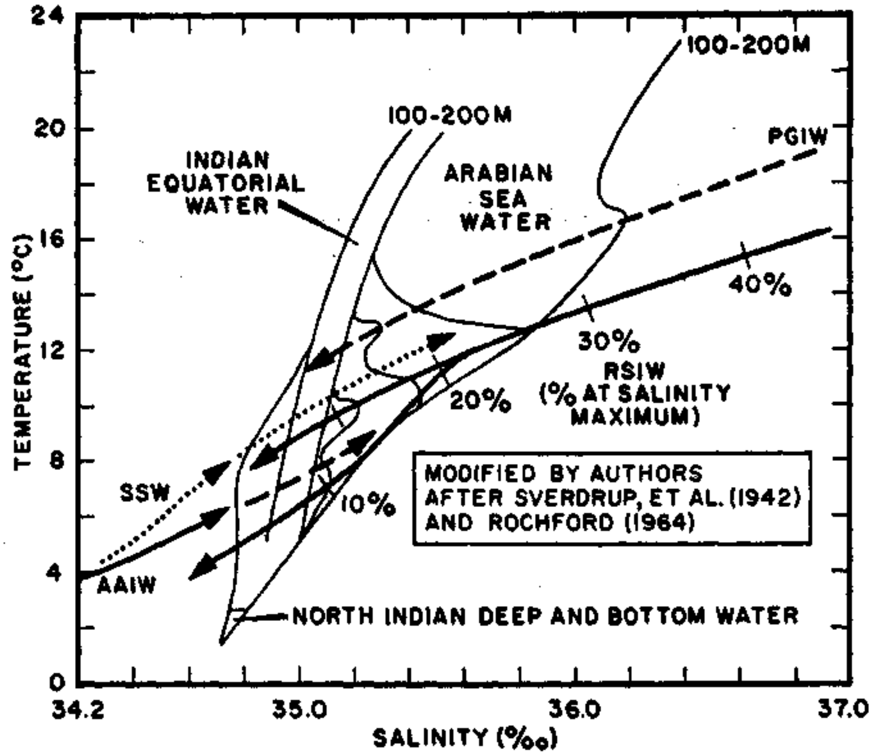

ABBREVIATIONS:
- AAIW = ANTARCTIC INTERMEDIATE WATER
- PGIW = PERSIAN GULF INTERMEDIATE WATER
- RSIW = RED SEA INTERMEDIATE WATER
- SSW = SUBTROPICAL SUBSURFACE WATER

Fig. 1. T-S relations in the northwest Indian Ocean.

North of about 8°N latitude, the predominate surface and near-surface water mass is Arabian Sea Water (ASW). This water mass has higher salinities and temperatures than those associated with IEW and takes the place of central water masses found in the North Atlantic and North Pacific Oceans. ASW apparently is formed by the excess of evaporation over precipitation found throughout the Arabian Sea and is reinforced by both RSIW and PGIW. ASW is confined to the Arabian Sea and the northern Arabian Basin by the North Equatorial Current during the northeast monsoon and by the Southwest Monsoon Current during the southwest monsoon.

The four intrusive water masses shown on Figure 1 (i.e., PGIW, SSW, RSIW, and AAIW) have been discussed previously. The percentage of RSIW present in the core layer (i.e., at the salinity maximum) can be determined using the RSIW

T-S curve shown on Figure 2. This curve was derived by the authors assuming a T-S value of 23°C-40.0‰ for 100% RSIW (Mamayav, 1969) and values of 8°C-34.8‰ and 4°C-34.6‰ for 0% RSIW on the upper and lower lobes, respectively. A RSIW concentration of approximately 20% marks the maximum limit of interfingering with AAIW observed by the authors. North Indian Deep and Bottom Water is found throughout the area at depths greater than 2000 to 2500 meters, and probably is a modified form of Antarctic Circumpolar Water (Sverdrup, *et al.*, 1942).

PRIMARY SOUND CHANNEL

Figures 2 and 3 show the annual average depth (in meters) and velocity (in meters/second) of the primary sound channel, respectively. An annual presentation was chosen for both parameters since monthly and seasonal variations in

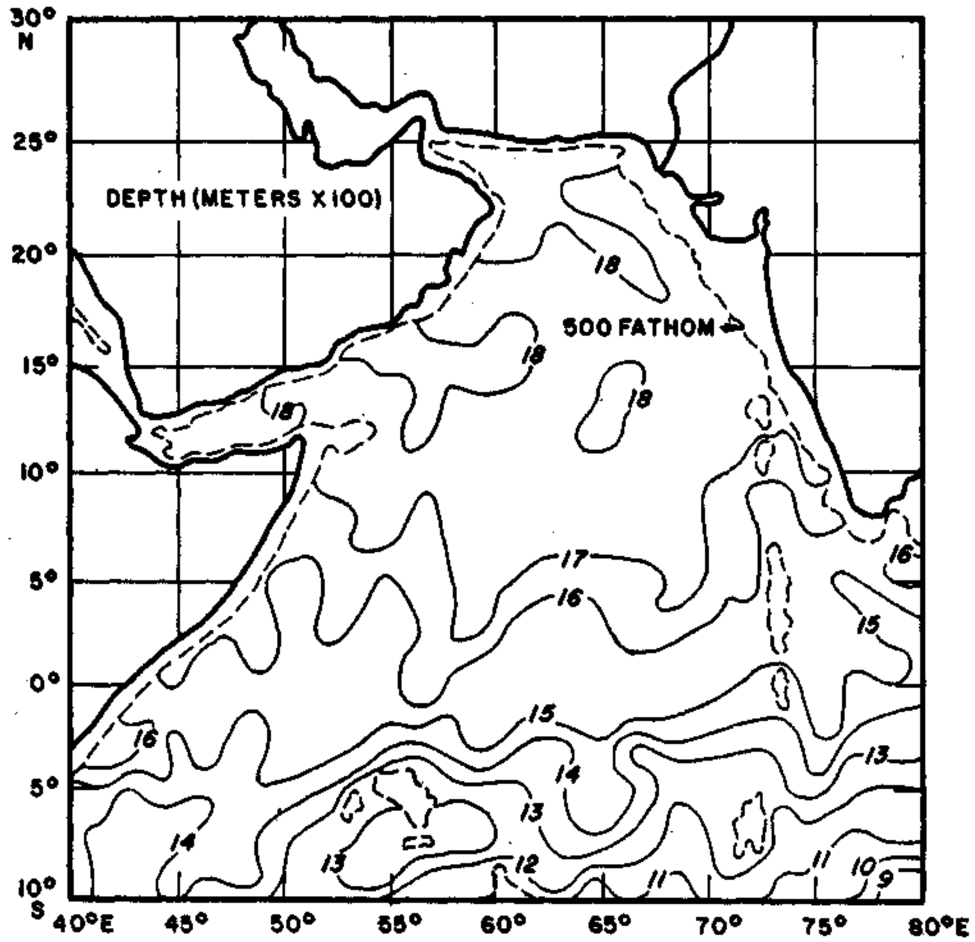

Fig. 2. Annual average depth of primary sound channel axis.

any given two-degree square were found to be as great as annual variations. Throughout the area, values of both parameters are anomalously large compared to values found at similar latitudes in the Pacific Ocean (Johnson and Norris, Apr. 1967). However, axial depths shown on Figure 2 are similar in magnitude to those found by the authors in the Northeast Atlantic Ocean between about 25° and 50°N latitude in the presence of large concentrations of Mediterranean Intermediate

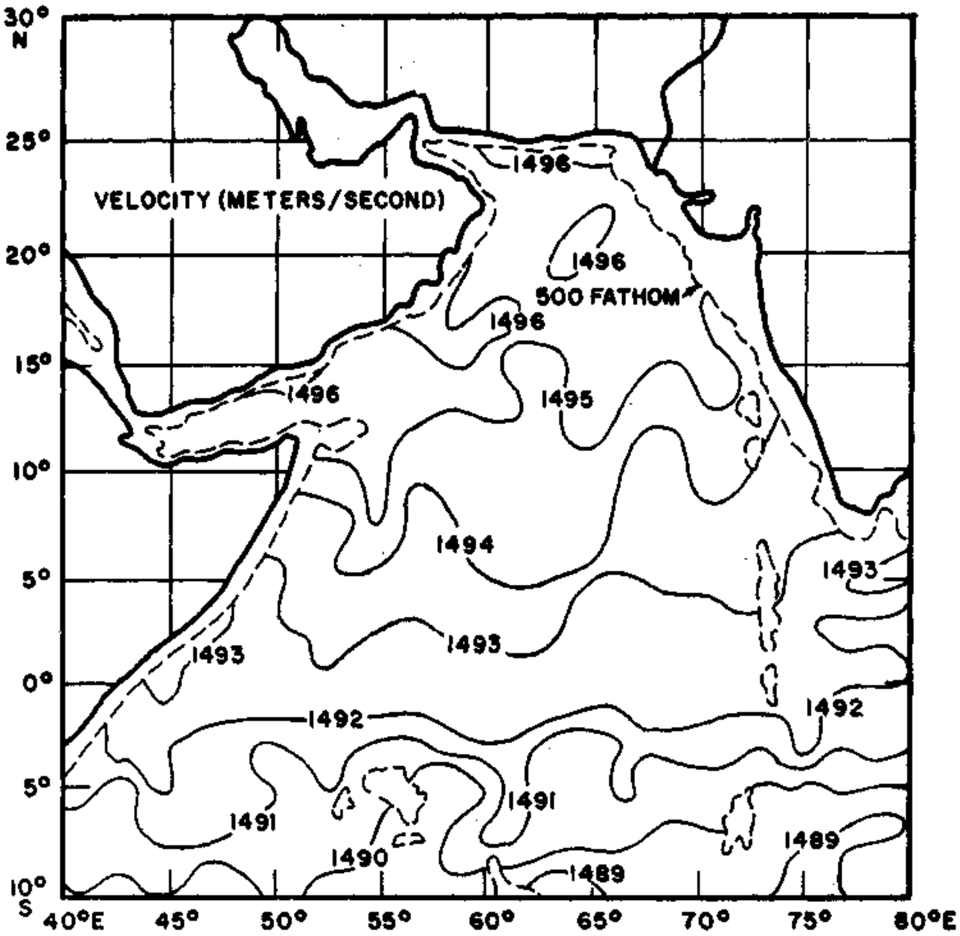

Fig. 3. Annual average velocity at primary sound channel axis.

Water (Fenner and Bucca, Dec. 1969). This indicates that high salinity RSIW and PGIW cause a pronounced increase in primary axial depth and primary axial velocity throughout the Northwest Indian Ocean. The greatest values of both parameters found in the area (greater than 1800 meters and greater than 1496 meters/second) lie in or in close proximity to the Gulf of Aden and the Gulf of Oman (Figs. A-1 and A-3). In contrast, the smallest values for both parameters (less than 1100 meters and less than 1489 meters/second) lie along the southern boundary of the area in a region influenced by relatively unmixed AAIW (Fig. A-8).

Axial depths greater than 1700 meters and axial velocities greater than 1494 meters/second are consistently found in the Gulf of Aden, Arabian Sea, and northern Arabian Basin (i.e., north of about 8°N latitude). The 1700-meter axial depth isoline shown on Figure 2 corresponds well to the northern extent of interfingering AAIW. The 8°N parallel also marks the southern limit of high salinity ASW. The marked southward tendency of the 1600- through 1800-meter axial depth isolines found in the northern Somali Basin (along about 55°E longitude) corresponds well to preferential flows of both RSIW and PGIW. This same tendency is observable in the 1493 to 1495-meter/second axial velocity isolines. The tight packing of the 1200- through 1500-meter axial depth isolines found south of the equator and east of the Seychelles-Mauritius Ridge corresponds well with the northern limit of relatively unmixed AAIW. A similar packing of axial velocity isolines is found in the same region.

Throughout most of the Somali, Arabian, and Mid-Indian Basins, the primary sound channel has a very broad structure (i.e., axial velocities vary by less than 1.0 meter/second from velocities found 300 to 500 meters above and below primary axial depth). Throughout these same regions, RSIW concentrations are less than 15% following dilution by interfingering AAIW and/or SSW. However, in the Arabian Sea, the primary sound channel is not as broad as that found farther to the south (compare Figs. A-2 and A-6). A broad primary sound channel also was found by the authors in the Northeast Atlantic Ocean south and west of the Canary Islands in the presence of diluted Mediterranean Intermediate Water (Fenner and Bucca, Dec. 1969). Therefore, it is concluded that broader primary sound channels are found in regions where diluted concentrations of high salinity water masses occur; whereas deeper primary sound channels are found in the presence of relatively unmixed high salinity water masses.

Sound Velocity Structures Above Primary Axial Depth

In the Northeast Atlantic, a widespread upper sound channel was found at the approximate depth of interaction of high salinity Mediterranean Intermediate Water with cooler, more dilute North Atlantic Central Water (Fenner and Bucca, Dec. 1969). In this same area, a subsurface sound velocity maximum was found at the approximate depth of the Mediterranean Intermediate Water high salinity core that lay at sound velocities from 2.0 to 15.0 meter/second greater than upper axial velocities. However, in the Northwest Indian Ocean, a widespread upper sound channel was not found (Fig. 4), despite the widespread presence of high salinity RSIW. Instead, the influences of high and low salinity intrusive water masses cause the formation of perturbations in the sound velocity structure at depths between approximately 200 meters (bottom of extremely strong negative sound velocity gradient) and primary axial depth. Figure 4 summarizes various statistics derived by the authors in an attempt to define the magnitude and areal extent of the limited upper sound channel and perturbations above primary axial depth found in the Northwest Indian Ocean.

A. *Perturbations Above Primary Axial Depth :*

Highly sporadic perturbations in the sound velocity structure above primary axial depth were found throughout most of the Northwest Indian Ocean, except in regions off the northwest Indian coast and in the southwest corner of the area (Figs. A-2 and A-8, respectively). Generally, minima were found associated

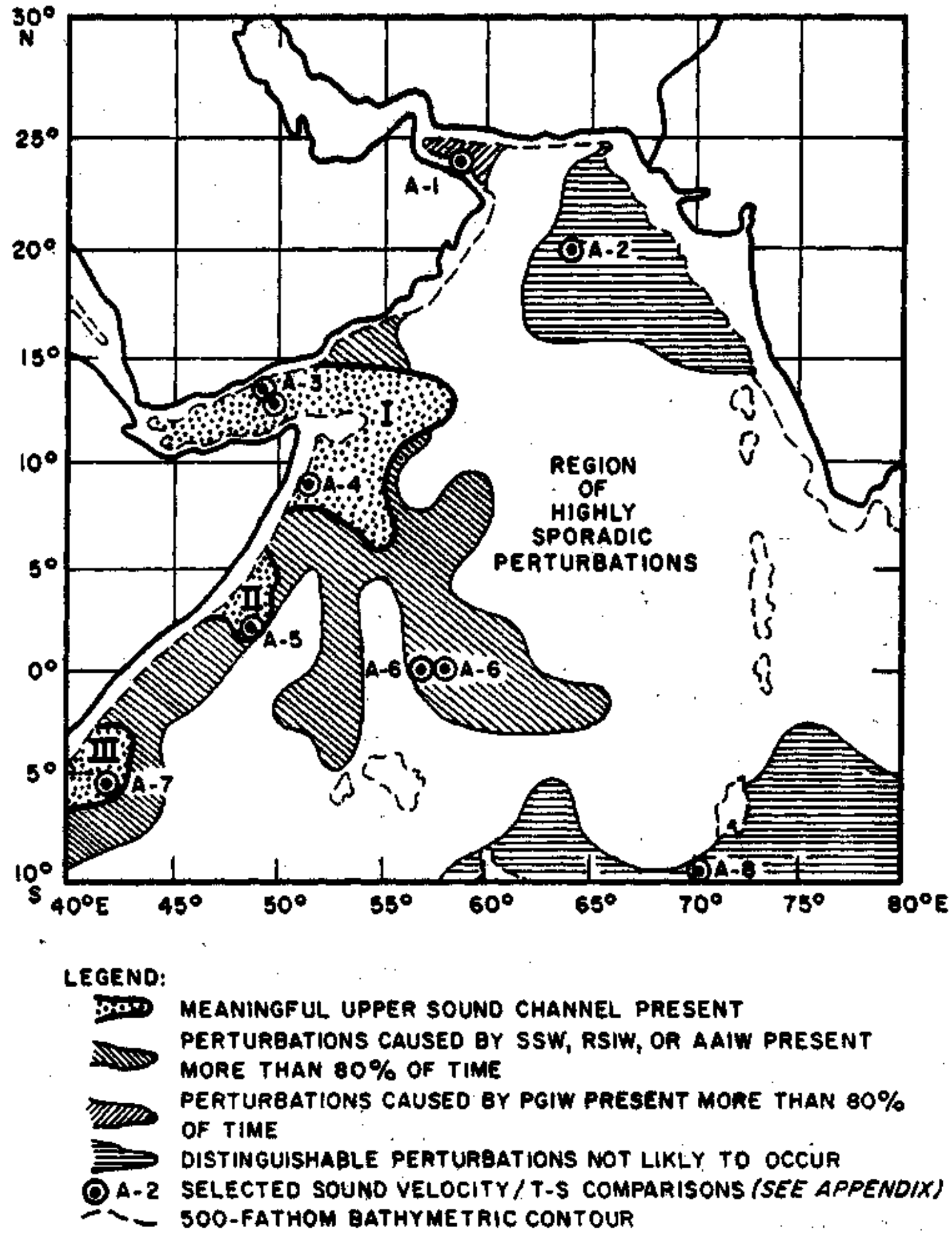

Fig. 4. Generalised occurrence of sound velocity perturbations above primary axial depth.

with either SSW or AAIW low salinity cores, whereas maxima were found at the approximate depth of the RSIW high salinity core. PGIW was found to have negligeable effects on the sound velocity structure except in the Gulf of Oman (Fig. A-1). This probably is due to the shallow depth of the PGIW high salinity core, which lies just below the strong thermocline and halocline encountered throughout most of the area. Perturbations were found to be sporadic in terms of temporal and spatial distribution as well as terms of magnitude throughout most of the area. However, in a region extending through the Gulf of Aden east to about 55°E longitude, south into the Somali Basin, and along the African coast perturbations were found to occur at least 80% of the time (during *both* monsoons). The several tongues that describe the outer limit of this region apparently correspond to various RSIW flows. The shape of the tongue lying due north of the Amirante Islands corresponds well with the shape of the 1600-meter axial depth isoline shown on Figure 2. This tongue probably is caused by a southward flow of RSIW bounded on either side by northward flows of interfingering AAIW. Figure A-6 shows representative sound velocity/T-S profiles for the region where perturbations occur more than 80% of the time. In this case, perturbations are found only during the northeast monsoon and only in association with interfingering RSIW and AAIW (despite the presence of SSW during both monsoons). However, in other cases, the authors noted the formation of perturbations in the presence of lesser concentrations of SSW during both monsoons. This discrepancy illustrates the sporadic nature of sound velocity perturbations found throughout large regions of the Northwest Indian Ocean, particularly in regions where low salinity and high salinity water masses are severely intermixed.

B. *Upper Sound Channel:*

A meaningful upper sound channel was found only in three limited regions of the Northwest Indian Ocean; the first extending through the Gulf of Aden and south and west of Socotra, a second along the Somali coast at about 5°N latitude, and a third northwest of Zanzibar. For purposes of this paper, a meaningful sound channel is defined as that sound velocity structure where upper axial velocity is at least 1.5 meters/second less than the velocity at the subsurface sound velocity maximum (roughly coincident with RSIW high salinity core). Upper sound channels are much better defined in the first region, particularly in the Gulf of Aden where differences between upper axial and subsurface maximum sound velocities can exceed 5.0 meters/second (Fig. A-3). In the second and third regions, absolute differences rarely exceed 3.5 meters/second and annual average differences in any two-degree square generally are less than 2.0 meters/second.

In the first region (Gulf of Aden and off Socotra), RSIW has relatively high concentrations (greater than 20%) and SSW has relatively high salinities (approximately 35.5°/₀₀) during both monsoons (Fig. A-3). An exception is found in the large upwelling centre off the Somali coast during the southwest monsoon (Fig. 10). The southwest monsoon profile shown on this figure is a good example of upwelling effects on the formation of an upper sound channel. Here, upwelling has lowered the SSW salinity to nearly 35.0°/₀₀, whereas RSIW has a concentration of only 16% (due to both the effects of upwelling and to a lesser flow of RSIW during the southwest monsoon). However the absolute difference in salinity between the SSW salinity minimum and the RSIW salinity maximum is greater during the southwest monsoon than during the northeast monsoon, leading to a better defined upper sound channel at 350 meters during the southwest monsoon. Interfingering AAIW is also found at this location during the southwest monsoon, leading to the formation of another channel at a depth of 700 meters. This channel is less defined than the channel at 350 meters and only occurs sporadically whenever cells of AAIW penetrate into this region. The formation of an upper sound channel in this first region therefore results from the intrusion of highly concentrated RSIW into a layer of well mixed SSW.

In the second region (off Somali coast at about 5°N latitude), both RSIW and SSW are relatively well mixed. RSIW has concentrations somewhat less than found in the first region (12% to 15%), while the SSW core salinity (approximately 35.0‰) is somewhat less saline than found farther north but more saline than found further south. Figure A-5 shows a good example of the upper sound channel structure encountered in this region during the southwest monsoon. During the northeast monsoon, upper sound channels in this region should be defined somewhat better due to higher concentrations of RSIW expected along the Somali coast. In fact, upper sound channels found in this region generally are as well defined or even better defined than those found south of Socotra, probably due to the presence of less saline SSW. This second region may be an extension of the region found in the Gulf of Aden and south of Socotra. However, it is felt that the mechanism for formation of an upper sound channel is different in this region than that postulated for the northern region. Apparently, an upper sound channel is formed here by the interaction of relatively well mixed RSIW and SSW, present in just the proper concentrations.

In the third region (northwest of Zanzibar), RSIW is well mixed (concentrations of approximately 10%) and SSW has relatively low salinities (approximately 34.8‰). Upper sound channels found in this region are better defined during both monsoons than those found anywhere in the area except in the Gulf of Aden due to the presence of relatively dilute SSW. Figure A-7 shows an extreme example of an upper sound channel found northwest of Zanzibar during the southwest monsoon. In this case, the interaction of low salinity SSW with well mixed RSIW has produced an upper sound channel at 350 meters with an axial velocity less than that found at the primary or deep axis (at about 1900 meters). In addition, interfingering AAIW and RSIW cause the formation of another sound velocity minimum at about 600 meters. Perturbations in the sound velocity profile between about 900 and 1800 meters apparently are related to the anomalously high salinities found below the RSIW core. In fact, sound velocities and salinities between about 700 and 1800 meters are anomalously high for this region. This anomaly probably is caused by the preferential flow of RSIW close to the African coast, the absence of AAIW at depths below 700 meters, and the presence of intense mixing associated with the formation of the Somali Current. The 1900-meter primary axial depth found on Figure A-7 indicates the presence of anomalously high salinity concentrations at intermediate depths, since average primary axial depths found in this region during both monsoons range between 1400 and 1600 meters (Fig. 2). However, other sound velocity and T-S profiles similar to Figure A-7 have been found northwest of Zanzibar during both monsoons. In the opinion of the authors, an upper sound channel is formed in this third region by intrusion of low salinity SSW into a layer of well mixed RSIW.

In summary, the various mechanisms for the existence or lack of a meaningful upper sound channel postulated above indicate the great complexity of sound velocity structures found above primary axial depth throughout the Northwest Indian Ocean. In the western Somali Basin, this complexity is increased by opposing flows of alternately high and low salinity intrusive water masses. The reader is cautioned that generalisations made in this paper on sound velocity structures between the permanent thermocline and primary axial depth are subject to revision upon collection of additional data, particularly in the Somali Basin during the northeast monsoon. However, it is felt that the absence of a widespread meaningful upper sound channel in the area is attributable to both the lack of high, unmixed concentrations of RSIW and to the lack of large quantities of cold, dilute water at depths above the RSIW core. In the Northeast Atlantic Ocean, the authors found that relatively cold, dilute North Atlantic Central Water and relatively warm, saline Mediterranean Intermediate Water were necessary for the formation of a well defined upper sound channel (Fenner and Bucca, Dec. 1969). No surface or near-surface sources of cold, dilute water are found in the Northwestern Indian Ocean except those associated with upwelling. The closest large source of cold dilute water in the Indian Ocean is at the Subtropical Convergence (about 40°S latitude) where SSW is formed. However, SSW is severely winnowed out north of the equator by PGIW above the RSIW below, and looses most of its cold and dilute characteristics prior to interacting with a relatively unmixed RSIW high salinity core. Therefore, the intensive mixing at intermediate depths found particularly in the Somali Basin during both monsoons ultimately is responsible for the lack of a widespread meaningful upper sound channel in the Northwest Indian Ocean.

Seasonal Critical Depths

Figures 5 and 6 show critical depths (in meters) for the northeast and southwest monsoons, respectively. Critical depths were derived using deep sound velocity curves constructed for Somali, Arabian, and Mid-Indian Basins. These average curves were derived from historical NODC sound velocity data and from deep T-S values of Olson (June 1968) (Computed by the equation of Wilson, 1960). Consistently higher average sound velocities were found in the Arabian Basin at depths above 4000 meters, indicating that the higher salinities and slightly higher temperatures found at shallower depths throughout both the Arabian Sea and the Arabian Basin persist throughout the water column.

During the northeast or winter monsoon, critical depths range from greater than 5200 meters in the region west of the Seychelles Islands to less than 4700 meters in the northern Arabian Sea. Critical depths in the Arabian Sea are shoaler during the northeast than during the southwest monsoon, mainly due to the effects of decreased surface insolation. Critical depths less than 4900 meters found in the northern end of the Arabian Sea correspond well with minima in sea surface temperature shown during December, January and February by La Violette and Frontenac (Aug. 1967). The northeast to southwest tendency of the 4900- and 5000-meter critical depth contours indicates the effects of the Northeast Monsoon Current which brings warmer and more saline water into the western Somali Basin. This mechanism leads to the deeper critical depths found north and west of the Seychelles Islands during the northeast monsoon. Also during this monsoon, warmer more saline waters from the southwestern Somali Basin are carried to the east across the area by the Equatorial Countercurrent. This results in the critical depths greater than 5100 meters found between the Chagos Archipelago and the Seychelles-Mauritius Ridge and to the east of the Maldive Islands. Critical depths less than 5100 meters shown in the southwest corner of the area on Figure 5 probably are related to the flow of the South Equatorial Current, whereas similar values found off the southern tip of India and west of the Maldive Islands indicate the influence of the North Equatorial Current.

During the southwest or summer monsoon, critical depths range from greater than 5200 meters in regions over the Carlsberg Ridge and northwest of the Laccadive Islands to less than 3500 meters in the strong upwelling center off the Somali coast. Upwelling off the Somali coast leads to the shoalest critical depths found in the Northwest Indian Ocean during the year (Fig. A-4). The effects of upwelling

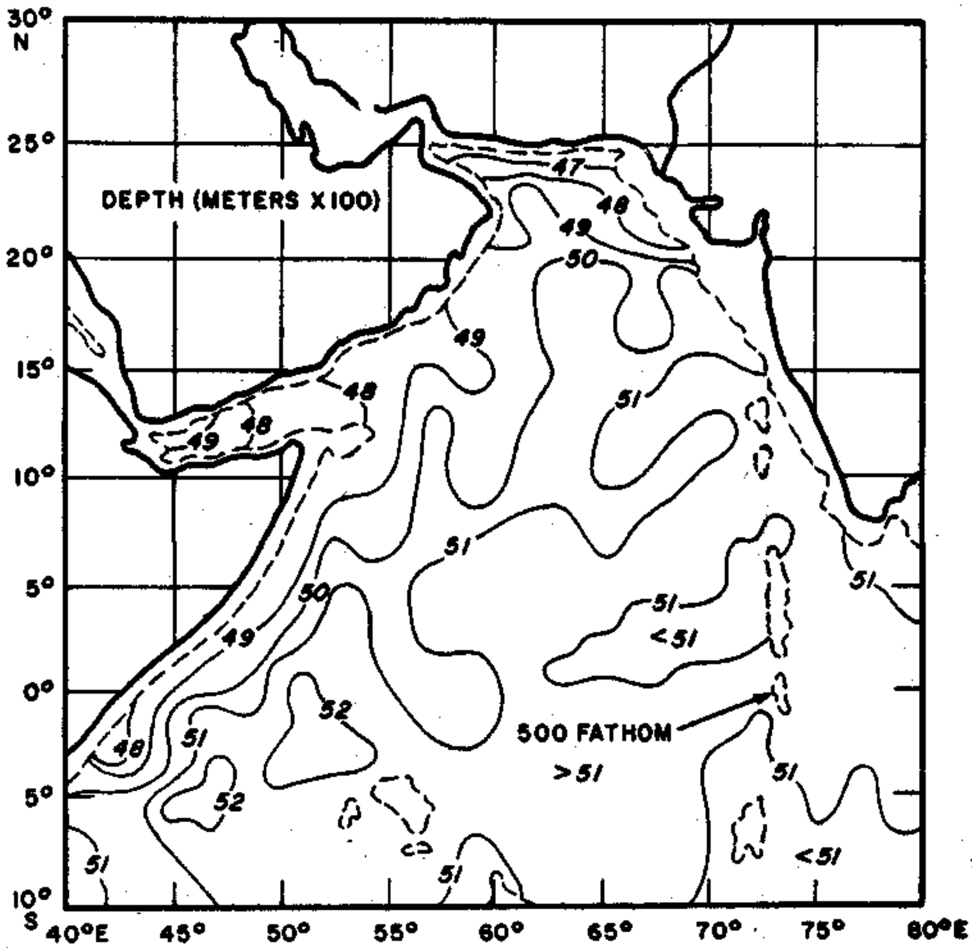

Fig. 5. Average critical depth for northeast monsoon (Nov.-April).

also are seen in the critical depth contours off the Muscat and Oman coasts (critical depths less than 4400 meters in upwelling center). However, despite the presence of upwelling along the western edge of the Arabian Sea, critical depths throughout this region are 100 to 300 meters deeper during the southwest monsoon due to increased surface insolation. The clockwise circulation of the Somali and Southwest Monsoon Currents is evident in the similar tendency of the 4800- through 5100-meter critical depth isolines found in the southern half of the area. The intense packing of critical depth isolines in the western Somali Basin is a result of both upwelling and an oceanic front associated with the eastern wall of the Somali Current. The large region with critical depths greater than 5100 meters found on both sides of the Carlsberg Ridge is also present during the northeast monsoon

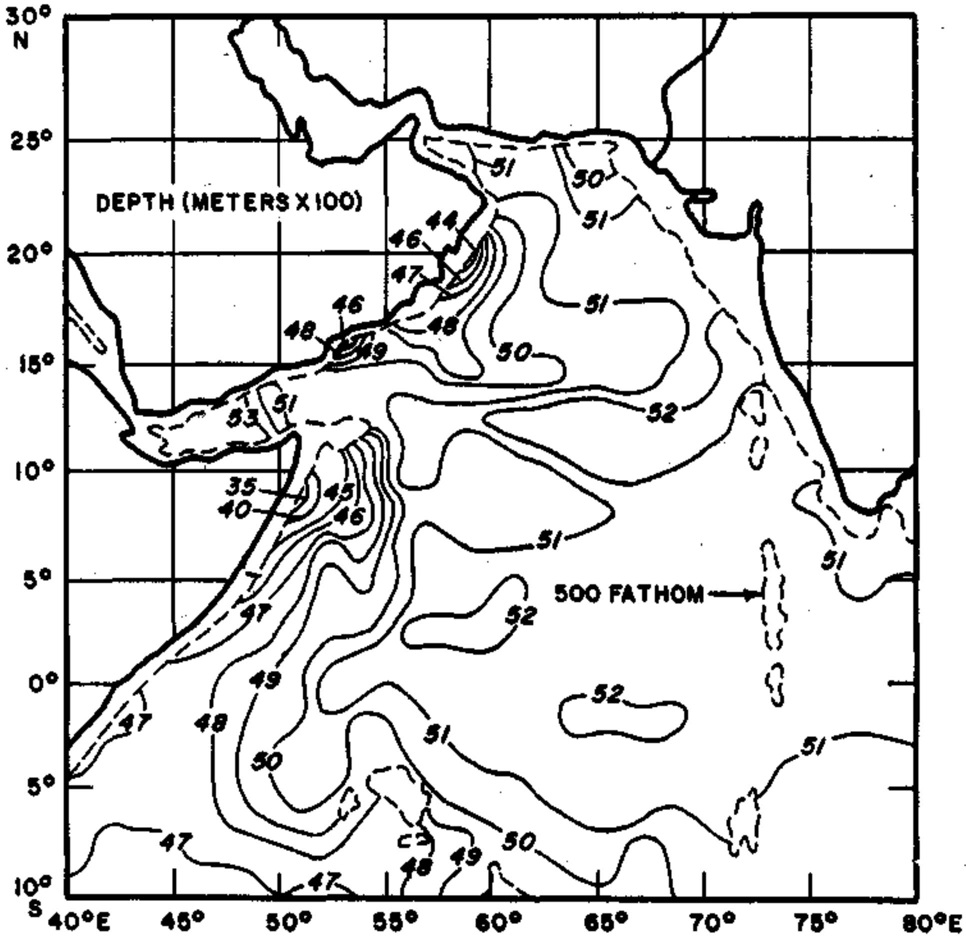

Fig. 6. Average critical depth for southwest monsoon (May-Oct.)

(compare Figs. 5 and 6). This indicates that the southern half of the area is equatorial throughout the year despite seasonally reversing monsoon winds and oceanic circulation.

References

FENNER, D. F. and BUCCA, P. J. 1969. The Upper and Deep Sound Channel in the Northeast Atlantic. *U. S. Naval Oceanographic Office Informal Report No.* 69 94 : 1-40.

IVANENKOV, V. N. and GUBIN, F. A. 1960. Water Masses and Hydrochemistry of the Western and Southern Parts of the Indian Ocean. *Transactions of the Marine Hydrophysical Institute Academy of Sciences,* USSR, **22** : 27-99 (translated from Russian by American Geophysical Union.)

JOHNSON, R. H. and NORRIS, R. A. 1967. Geographic Variation in SOFAR Speed and Axis Depth in the Pacific. *Hawaii Institute of Geophysics Report No.* 67 7 : 1-93.

LA VIOLETTE, R. H. and FRONTENAC, T. R. 1967. Temperature, Salinity, and Density of the World's Seas : Arabian Sea, Persian Gulf, and Red Sea. *U.S. Naval Oceanographic Office Informal Report No.* 67 **49** : 1-111.

MAMAYAV, O. I. 1969. Generalised T-S Diagrams of the Water Masses of the World Oceans. *Oceanology, Academy of Sciences, U.S.S.R.* 9(1) : 49-55 (translated from Russian by American Geophysical Union).

MATTHEWS, S.W. 1967. Science Explores the Monsoon Sea. *National Geographic*, **132** (4) : 554-575.

OLSON, B. E. 1968. *On the Abyssal Temperatures of the World Oceans.* Oregon State University, Ph.D. Thesis. 151 pp.

ROCHFORD, D. J. 1964. Salinity Maximum in the Upper 1000 Meters of the North Indian Ocean. *Australian Journal of Marine and Freshwater Research*, **15** (1) : 1-24.

——— 1966. Source Regions of Oxygen Maxima in Intermediate Depths of the Arabian Sea. *Ibid.*, **17** : 1-30.

RYTHER, J. H. and MENZEL, D. W. 1965. On Production, Composition, and Distribution of Organic Matter in the Western Arabian Sea. *Deep-Sea Research*, **12** : 199-209.

SHCHERBININ, A. D. 1969. Water Structure of the Equatorial Indian Ocean. *Oceanology, Academy of Sciences, U.S.S.R.*, 9 (4) : 487-495 (translated from Russian by American Geophysical Union).

SVERDRUP, H. U., JOHNSON, M. W. and FLEMING, R. H. 1942. *The Oceans—Their Physics, Chemistry, and General Biology.* Prentice-Hall, Inc., Englewood Cliffs, N.J., 1060 pp.

SWALLOW, J. C. and BRUCE, J. G. 1966. Current Measurements off the Somali Coast during the Southwest Monsoon of 1964. *Deep-Sea Research*, **13** : 861-868.

WARREN, B., STOMMEL, H. and SWALLOW, J. C. 1966. Water Masses and Patterns of Flow in the Somali Basin during the Southwest Monsoon of 1964. *Ibid.*, **13** : 825-860.

WILSON, W. D. 1960. Equation of the Speed of Sound in Sea Water. *Journal of the Acoustical Society of America*, **13** (10) : 1357.

APPENDIX

SELECTED SOUND VELOCITY/T-S COMPARISONS

All sound velocity profiles shown on Figures A-1 through A-8 were derived according to the equation of Wilson (1960). These profiles were available to the authors from NODC data listings of various IIOE cruises. Any given sound velocity/T-S comparison shown herein was derived from the same single oceanographic observation. No averaging processes were used in the construction of any of the profiles. Therefore, the selected profiles are not typical for any specific region, but only show general trends encountered throughout the area.

All sound velocity profiles shown on the following pages extend deeper than primary axial depth except for the northeast monsoon profiles shown on Figures A-3 and A-4. Each of these profiles represents part of a seasonal comparison, and in each case southwest monsoon sound velocity profiles deeper than primary axial depth also are shown. All sound velocity and T-S profiles shown herein are drawn only to the maximum depth of actual data. To facilitate comparison between sound velocity and T-S profiles, the following legend has been devised :

A : depth of Red Sea Intermediate Water (RSIW) absolute salinity maximum

A^1: depth of second RSIW high salinity lobe (in cases of interfingering, when present)

B : depth of Subtropical Subsurface Water (SSW) salinity minimum

C : depth of Antarctic Intermediate Water (AAIW) salinity minimum

D : depth of Persian Gulf Intermediate Water (PGIW) salinity maximum

E : depth of a salinity maximum caused by mixing of RSIW and PGIW.

Concentrations of RSIW (in percent) are given only for the absolute RSIW salinity maximum ('A' notation above).

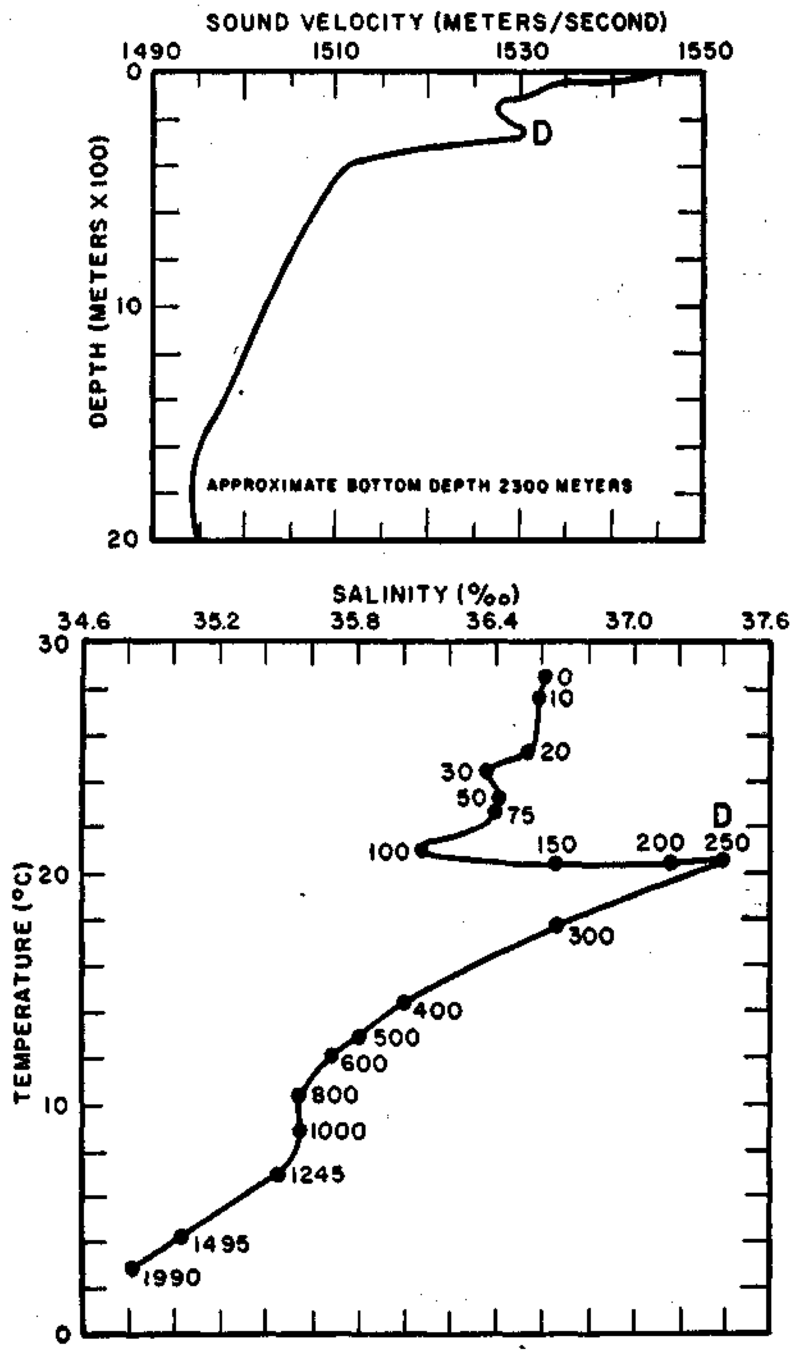

Fig. A-1. Selected sound velocity/T-S comparison for southwest monsoon.

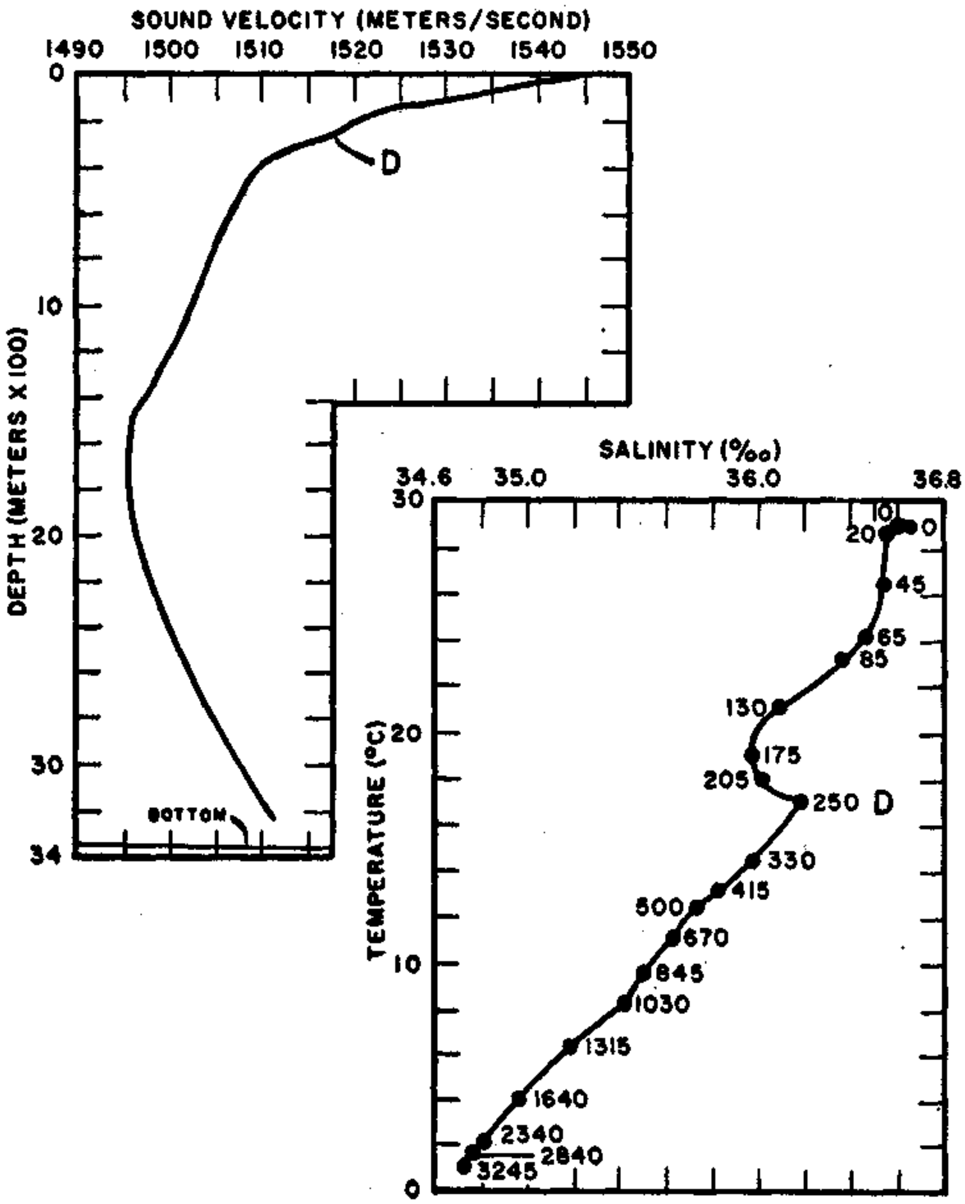

Fig. A-2. Selected sound velocity/T-S comparison for southwest monsoon.

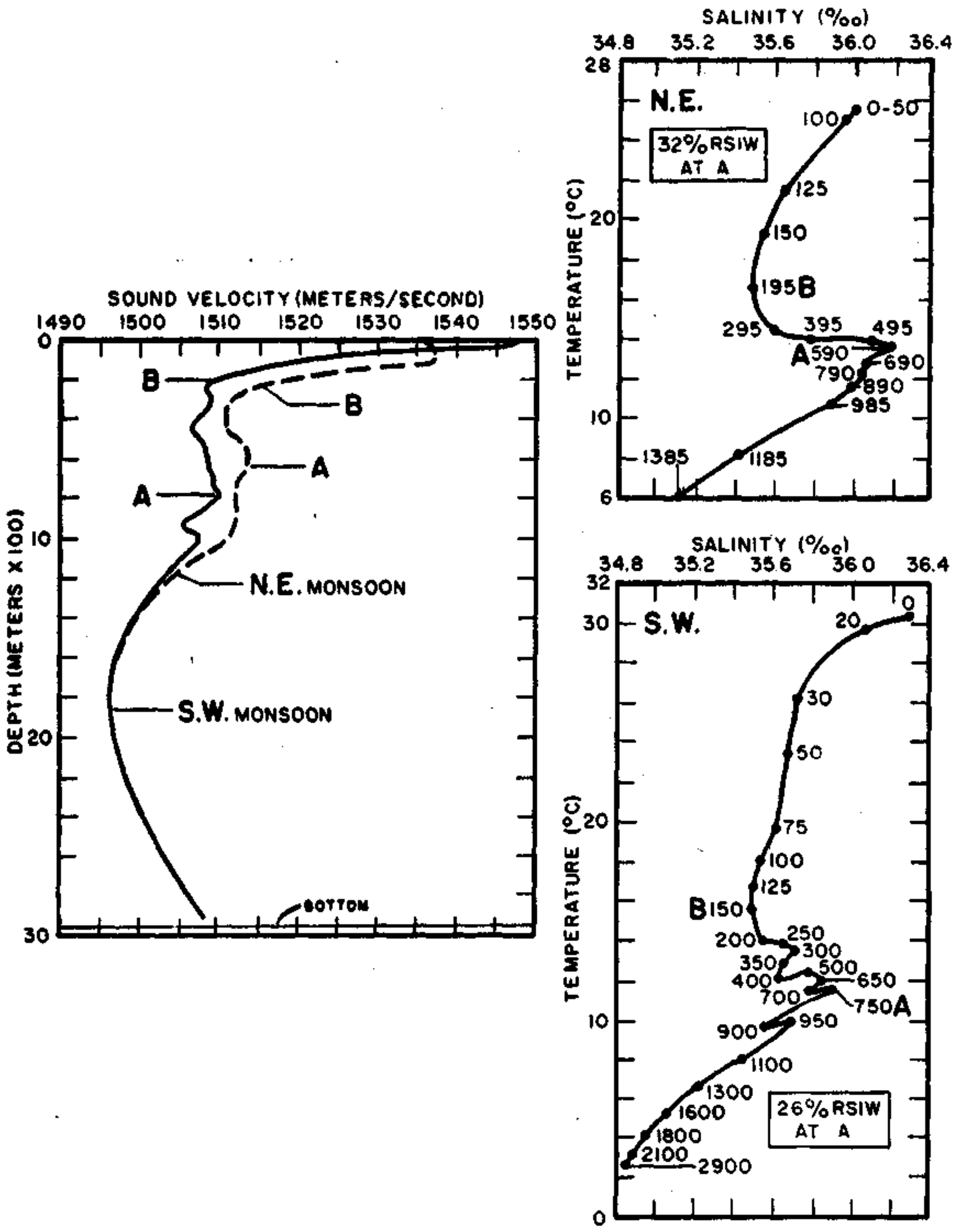

Fig. A-3. Selected seasonal sound velocity/T-S comparison.

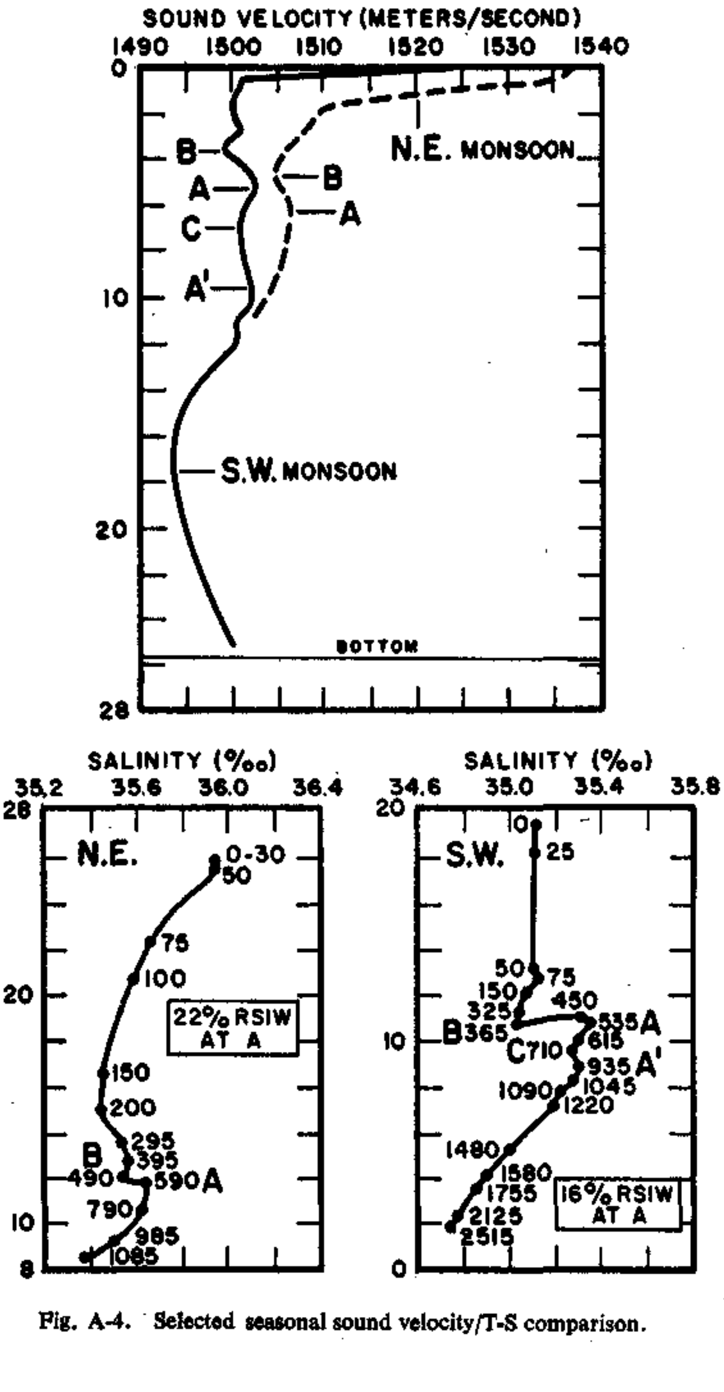

Fig. A-4. Selected seasonal sound velocity/T-S comparison.

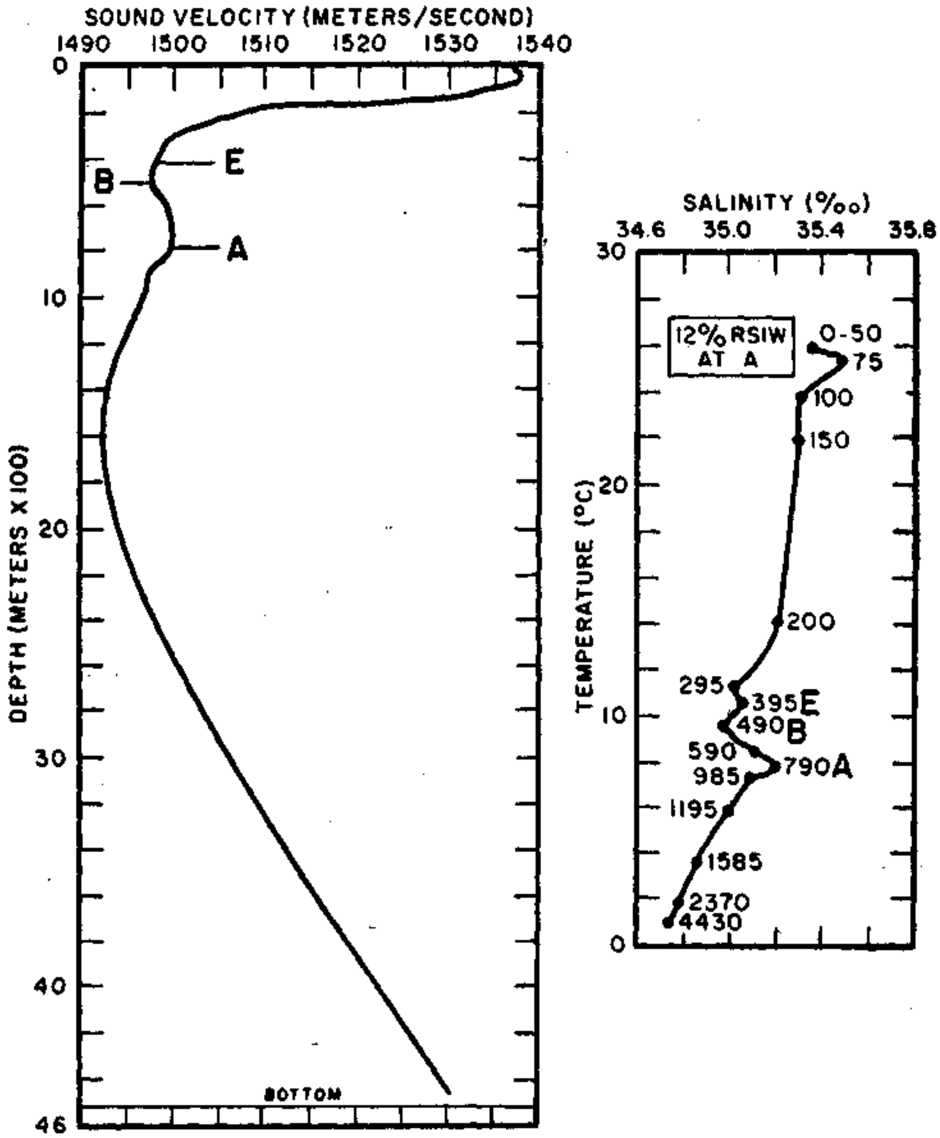

Fig. A-5. Selected sound velocity/T-S comparison for southwest monsoon.

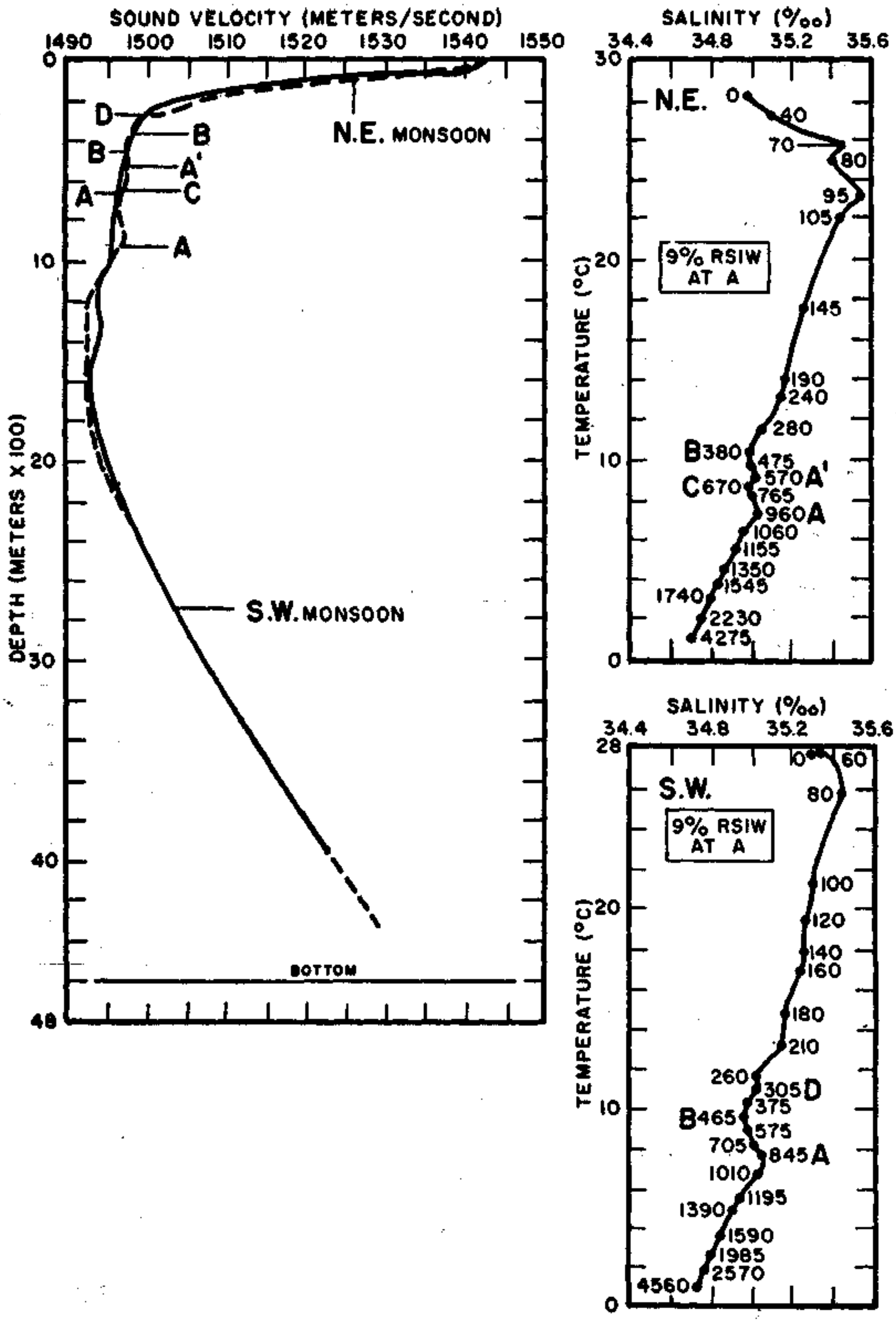

Fig. A-6. Selected seasonal sound velocity/T-S comparison.

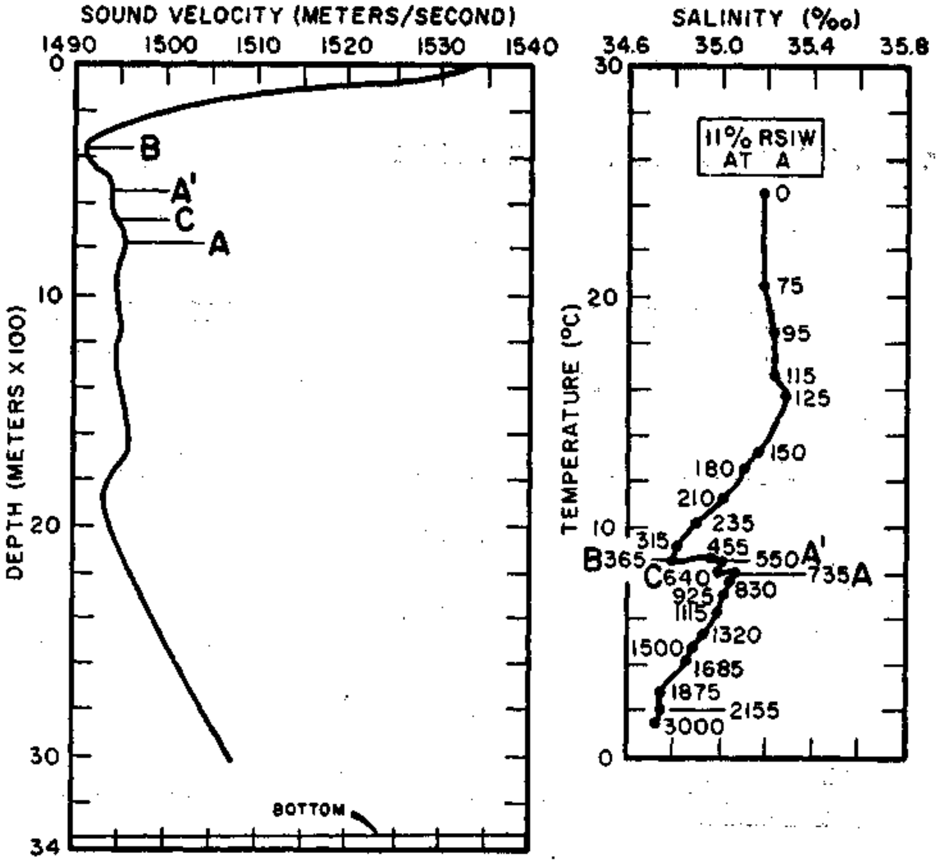

Fig. A-7. Selected sound velocity/T-S comparison for southwest monsoon.

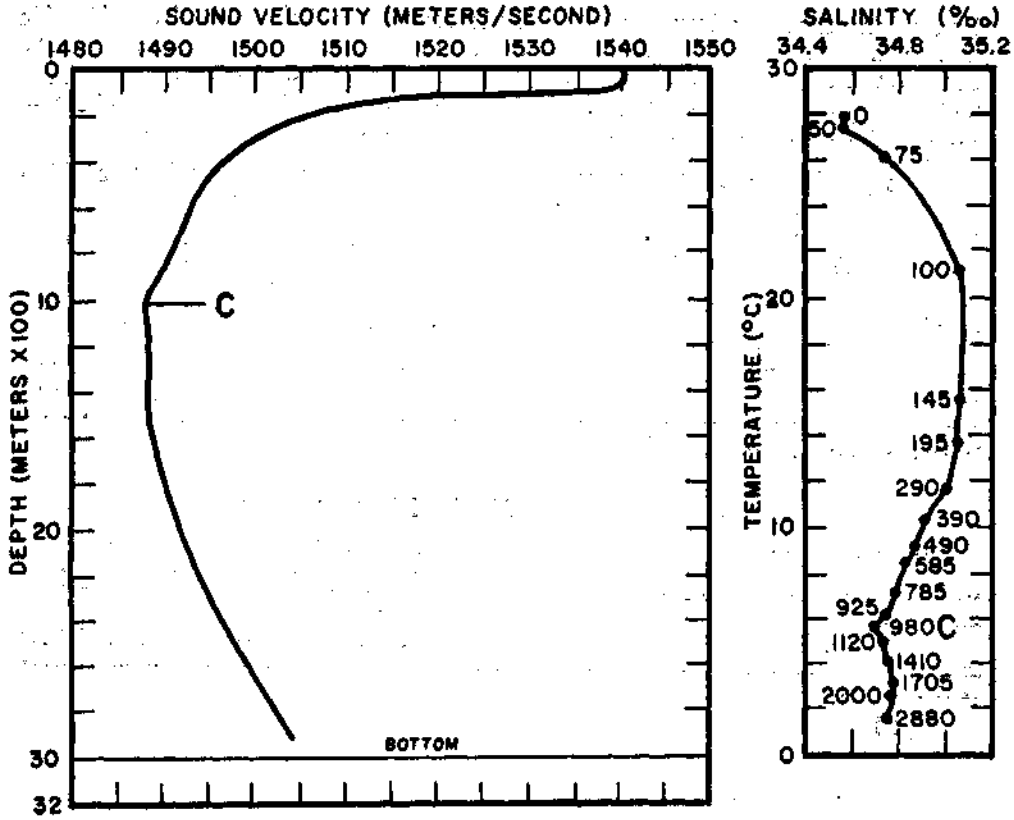

Fig. A-8. Selected sound velocity/T-S comparison for northeast monsoon.